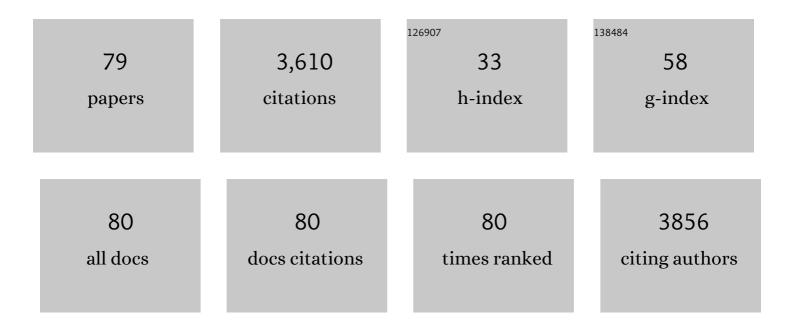
List of Publications by Year in descending order

Source: https://exaly.com/author-pdf/8248620/publications.pdf Version: 2024-02-01



Ρυσαι Μλαίο

#	Article	IF	CITATIONS
1	Aerosol optical properties and their radiative effects in northern China. Journal of Geophysical Research, 2007, 112, .	3.3	209
2	A simple method to estimate actual evapotranspiration from a combination of net radiation, vegetation index, and temperature. Journal of Geophysical Research, 2007, 112, .	3.3	200
3	Aerosol optical depth (AOD) and Ãngström exponent of aerosols observed by the Chinese Sun Hazemeter Network from August 2004 to September 2005. Journal of Geophysical Research, 2007, 112, .	3.3	166
4	Estimation of surface long wave radiation and broadband emissivity using Moderate Resolution Imaging Spectroradiometer (MODIS) land surface temperature/emissivity products. Journal of Geophysical Research, 2005, 110, .	3.3	164
5	Validation of SO <sub>2</sub> retrievals from the Ozone Monitoring Instrument over NE China. Journal of Geophysical Research, 2008, 113, .	3.3	139
6	Influences of urbanization on surface characteristics as derived from the Moderateâ€Resolution Imaging Spectroradiometer: A case study for the Beijing metropolitan area. Journal of Geophysical Research, 2007, 112, .	3.3	137
7	Chemical characterization of air pollution in Eastern China and the Eastern United States. Atmospheric Environment, 2006, 40, 2607-2625.	4.1	134
8	Aerosol optical properties and radiative effects in the Yangtze Delta region of China. Journal of Geophysical Research, 2007, 112, .	3.3	120
9	The Campaign on Atmospheric Aerosol Research Network of China: CARE-China. Bulletin of the American Meteorological Society, 2015, 96, 1137-1155.	3.3	115
10	Baseline continental aerosol over the central Tibetan plateau and a case study of aerosol transport from South Asia. Atmospheric Environment, 2011, 45, 7370-7378.	4.1	112
11	Validation and understanding of Moderate Resolution Imaging Spectroradiometer aerosol products (C5) using groundâ€based measurements from the handheld Sun photometer network in China. Journal of Geophysical Research, 2007, 112, .	3.3	108
12	Variation of surface albedo and soil thermal parameters with soil moisture content at a semi-desert site on the western Tibetan Plateau. Boundary-Layer Meteorology, 2005, 116, 117-129.	2.3	93
13	Aerosol characterization over the North China Plain: Haze life cycle and biomass burning impacts in summer. Journal of Geophysical Research D: Atmospheres, 2016, 121, 2508-2521.	3.3	93
14	In situ measurements of trace gases and aerosol optical properties at a rural site in northern China during East Asian Study of Tropospheric Aerosols: An International Regional Experiment 2005. Journal of Geophysical Research, 2007, 112, .	3.3	91
15	Seasonal variations in aerosol optical properties over China. Journal of Geophysical Research, 2011, 116, .	3.3	87
16	Improved aerosol correction for OMI tropospheric NO <sub>2</sub> retrieval over East Asia: constraint from CALIOP aerosol vertical profile. Atmospheric Measurement Techniques, 2019, 12, 1-21.	3.1	75
17	Aerosol optical depth over the Tibetan Plateau and its relation to aerosols over the Taklimakan Desert. Geophysical Research Letters, 2008, 35, .	4.0	72
18	Low-level temperature inversions and their effect on aerosol condensation nuclei concentrations under different large-scale synoptic circulations. Advances in Atmospheric Sciences, 2015, 32, 898-908.	4.3	72

#	Article	IF	CITATIONS
19	Vertical profiles of black carbon measured by a micro-aethalometer in summer in the North China Plain. Atmospheric Chemistry and Physics, 2016, 16, 10441-10454.	4.9	72
20	Positive relationship between liquid cloud droplet effective radius and aerosol optical depth over Eastern China from satellite data. Atmospheric Environment, 2014, 84, 244-253.	4.1	66
21	TROPOMI–Sentinel-5 Precursor formaldehyde validation using an extensive network of ground-based Fourier-transform infrared stations. Atmospheric Measurement Techniques, 2020, 13, 3751-3767.	3.1	66
22	Climatological aspects of aerosol optical properties in North China Plain based on ground and satellite remote-sensing data. Journal of Quantitative Spectroscopy and Radiative Transfer, 2013, 127, 12-23.	2.3	60
23	Identification of sources and formation processes of atmospheric sulfate by sulfur isotope and scanning electron microscope measurements. Journal of Geophysical Research, 2010, 115, .	3.3	58
24	Significant reduction of surface solar irradiance induced by aerosols in a suburban region in northeastern China. Journal of Geophysical Research, 2007, 112, .	3.3	57
25	Validation of methane and carbon monoxide from Sentinel-5 Precursor using TCCON and NDACC-IRWG stations. Atmospheric Measurement Techniques, 2021, 14, 6249-6304.	3.1	57
26	Trends in aerosol optical properties over the Bohai Rim in Northeast China from 2004 to 2010. Atmospheric Environment, 2011, 45, 6317-6325.	4.1	56
27	Comparison and Validation of TROPOMI and OMI NO2 Observations over China. Atmosphere, 2020, 11, 636.	2.3	49
28	Diurnal variability of dust aerosol optical thickness and Angström exponent over dust source regions in China. Geophysical Research Letters, 2004, 31, .	4.0	47
29	Growth rates of fine aerosol particles at a site near Beijing in June 2013. Advances in Atmospheric Sciences, 2018, 35, 209-217.	4.3	45
30	Spatial and temporal changes in SO <sub>2</sub> regimes over China in the recent decade and the driving mechanism. Atmospheric Chemistry and Physics, 2018, 18, 18063-18078.	4.9	44
31	Impacts of organic aerosols and its oxidation level on CCN activity from measurement at a suburban site in China. Atmospheric Chemistry and Physics, 2016, 16, 5413-5425.	4.9	42
32	Comparison between measurements and modeling of UV-B irradiance for clear sky: a case study. Applied Optics, 1994, 33, 3964.	2.1	41
33	The Spatial–Temporal Variation of Tropospheric NO2 over China during 2005 to 2018. Atmosphere, 2019, 10, 444.	2.3	39
34	Studying the pollution of Moscow and Beijing atmospheres with carbon monoxide and aerosol. Izvestiya - Atmospheric and Oceanic Physics, 2015, 51, 1-11.	0.9	32
35	Validation of an UV inversion algorithm using satellite and surface measurements. Journal of Geophysical Research, 2000, 105, 5037-5048.	3.3	31
36	A simple and efficient method for retrieving surface UV radiation dose rate from satellite. Journal of Geophysical Research, 2000, 105, 5027-5036.	3.3	30

#	Article	IF	CITATIONS
37	Validation of MODIS aerosol products by CSHNET over China. Science Bulletin, 2007, 52, 1708-1718.	1.7	30
38	Validation of TANSO-FTS/GOSAT XCO <sub>2</sub> and XCH <sub>4</sub> glint mode retrievals using TCCON data from near-ocean sites. Atmospheric Measurement Techniques, 2016, 9, 1415-1430.	3.1	30
39	CFC-11, CFC-12 and HCFC-22 ground-based remote sensing FTIR measurements at Réunion Island and comparisons with MIPAS/ENVISAT data. Atmospheric Measurement Techniques, 2016, 9, 5621-5636.	3.1	29
40	New ground-based Fourier-transform near-infrared solar absorption measurements of XCO <sub>2</sub> , XCH <sub>4</sub> and XCO at Xianghe, China. Earth System Science Data, 2020, 12, 1679-1696.	9.9	28
41	Midlatitude cirrus cloud radiative forcing over China. Journal of Geophysical Research, 2010, 115, .	3.3	25
42	In situ measurements of aerosol mass concentration and radiative properties in Xianghe, southeast of Beijing. Journal of Geophysical Research, 2007, 112, .	3.3	24
43	Advances in sunphotometer-measured aerosol optical properties and related topics in China: Impetus and perspectives. Atmospheric Research, 2021, 249, 105286.	4.1	23
44	Change of NO2 column density over Beijing from satellite measurement during the Beijing 2008 Olympic Games. Science Bulletin, 2010, 55, 308-313.	1.7	21
45	Long-Term Trends of Carbon Monoxide Total Columnar Amount in Urban Areas and Background Regions: Ground- and Satellite-based Spectroscopic Measurements. Advances in Atmospheric Sciences, 2018, 35, 785-795.	4.3	21
46	Analysis of Low-level Temperature Inversions and Their Effects on Aerosols in the Lower Atmosphere. Advances in Atmospheric Sciences, 2019, 36, 1235-1250.	4.3	21
47	Observed decreases in on-road CO <sub>2</sub> concentrations in Beijing during COVID-19 restrictions. Atmospheric Chemistry and Physics, 2021, 21, 4599-4614.	4.9	21
48	Aerosol chemistry and particle growth events at an urban downwind site in North China Plain. Atmospheric Chemistry and Physics, 2018, 18, 14637-14651.	4.9	19
49	The aerosol direct radiative forcing over the Beijing metropolitan area from 2004 to 2011. Journal of Aerosol Science, 2014, 69, 62-70.	3.8	18
50	New dust aerosol identification method for spaceborne lidar measurements. Journal of Quantitative Spectroscopy and Radiative Transfer, 2011, 112, 338-345.	2.3	17
51	Cirrus cloud macrophysical and optical properties over North China from CALIOP measurements. Advances in Atmospheric Sciences, 2011, 28, 653-664.	4.3	14
52	Nocturnal aerosol particle formation in the North China Plain. Lithuanian Journal of Physics, 2015, 55,	0.4	13
53	Effects of ocean particles on the upwelling radiance and polarized radiance in the atmosphere-ocean system. Advances in Atmospheric Sciences, 2015, 32, 1186-1196.	4.3	12
54	Assessment of the Performance of TROPOMI NO2 and SO2 Data Products in the North China Plain: Comparison, Correction and Application. Remote Sensing, 2022, 14, 214.	4.0	12

#	Article	IF	CITATIONS
55	XCO2 satellite retrieval experiments in short-wave infrared spectrum and ground-based validation. Science China Earth Sciences, 2015, 58, 1191-1197.	5.2	11
56	Ground-based FTIR retrievals of SF <sub>6</sub> on Reunion Island. Atmospheric Measurement Techniques, 2018, 11, 651-662.	3.1	11
57	Estimation of PM2.5 Mass Concentration from Visibility. Advances in Atmospheric Sciences, 2020, 37, 671-678.	4.3	11
58	Ground-based measurements of aerosol optical properties and radiative forcing in North China. Particuology: Science and Technology of Particles, 2007, 5, 202-205.	0.4	10
59	Global to local impacts on atmospheric CO <sub>2</sub> from the COVID-19 lockdown, biosphere and weather variabilities. Environmental Research Letters, 2022, 17, 015003.	5.2	10
60	Deriving Temporal and Vertical Distributions of Methane in Xianghe Using Ground-based Fourier Transform Infrared and Gas-analyzer Measurements. Advances in Atmospheric Sciences, 2020, 37, 597-607.	4.3	9
61	Spatial and temporal variations of CO <sub>2</sub> mole fractions observed at Beijing, Xianghe, and Xinglong in North China. Atmospheric Chemistry and Physics, 2021, 21, 11741-11757.	4.9	9
62	Ground-based Fourier transform infrared (FTIR) O <sub>3</sub> retrievals from the 3040 cm <sup>â^1</sup> spectral range at Xianghe, China. Atmospheric Measurement Techniques, 2020, 13, 5379-5394.	3.1	9
63	Oscillation cumulative volatile organic compounds on the northern edge of the North China Plain: Impact of mountain-plain breeze. Science of the Total Environment, 2022, 821, 153541.	8.0	9
64	Surface and Column-Integrated Aerosol Properties of Heavy Haze Events in January 2013 over the North China Plain. Aerosol and Air Quality Research, 2015, 15, 1514-1524.	2.1	8
65	CHANGES IN TRENDS OF ATMOSPHERIC COMPOSITION OVER URBAN AND BACKGROUND REGIONS OF EURASIA: ESTIMATES BASED ON SPECTROSCOPIC OBSERVATIONS. Geography, Environment, Sustainability, 2018, 11, 84-96.	1.3	7
66	Glyoxal tropospheric column retrievals from TROPOMI – multi-satellite intercomparison and ground-based validation. Atmospheric Measurement Techniques, 2021, 14, 7775-7807.	3.1	7
67	Recent progress in atmospheric observation research in China. Advances in Atmospheric Sciences, 2007, 24, 940-953.	4.3	6
68	A New Method to Calibrate Shortwave Solar Radiation Measurements. Journal of Atmospheric and Oceanic Technology, 2014, 31, 1321-1329.	1.3	6
69	Characterization of Regional Combustion Efficiency using ΔXCO: ΔXCO2 Observed by a Portable Fourier-Transform Spectrometer at an Urban Site in Beijing. Advances in Atmospheric Sciences, 2022, , 1-17.	4.3	6
70	Re-examine the APEC blue in Beijing 2014. Journal of Atmospheric Chemistry, 2018, 75, 235-246.	3.2	5
71	<title>Preliminary accuracy assessment of MODIS land surface temperature products at a semi-desert site</title> ., 2005,,.		4
72	In-situ measurement of CO2 at the Xinglong regional background station over North China. Atmospheric and Oceanic Science Letters, 2019, 12, 385-391.	1.3	4

#	Article	IF	CITATIONS
73	Correction to "Aerosol optical properties and their radiative effects in northern China― Journal of Geophysical Research, 2008, 113, .	3.3	3
74	Radiative Transfer Model Simulations for Ground-Based Microwave Radiometers in North China. Remote Sensing, 2021, 13, 5161.	4.0	3
75	Tropospheric and stratospheric NO retrieved from ground-based Fourier-transform infrared (FTIR) measurements. Atmospheric Measurement Techniques, 2021, 14, 6233-6247.	3.1	2
76	Preliminary comparison of OMI PBL SO2 data to in-situ measurements in Beijing. , 2008, , .		1
77	Measurement and analysis of atmospheric aerosol optical thickness and Angstrom exponent of 1998-2000 over the Beijing area. , 2003, , .		0
78	<title>Ground-based monitoring of CO and H&lt;formula&gt;&lt;inf&gt;&lt;roman&gt;2&lt;/roman&gt;&lt;/inf&gt;&lt;/formula&gt;O total content in the atmosphere over Beijing</title> . , 2005, 5832, 316.		0
79	Calibration and Data Quality Assurance Technical Advancements for Quantitative Remote Sensing in the DRAGON 4 Project. Remote Sensing, 2021, 13, 4996.	4.0	0